Clin Neuroradiol (2019) 29:523–532
https://doi.org/10.1007/s00062-018-0686-0

ORIGINAL ARTICLE

Cervical Spine Prospective Feasibility Study

Dynamic Flexion-Extension Diffusion-Tensor Weighted Magnetic Resonance Imaging

Bawarjan Schatlo[1,2,3] · Luca Remonda[1] · Philipp Gruber[4] · Javier Fandino[2] · Veit Rohde[3] · Ali-Reza Fathi[5] · Jatta Berberat[1]

Received: 22 January 2018 / Accepted: 30 March 2018 / Published online: 18 April 2018

Abstract

Purpose Diffusion tensor imaging (DTI) in flexion-extension may serve as a diagnostic tool to improve the sensitivity for detection of myelopathy. In this study, the feasibility and reproducibility of dynamic DTI in the cervical spinal cord was assessed in healthy volunteers and patients.

Methods All subjects were examined in maximum neck flexion-extension in a 3T magnetic resonance imaging (MRI) scanner. Range of motion, space available for the spinal cord, fractional anisotropy (FA) and apparent diffusion coefficient (ADC) were measured and compared between the neck positions.

Results Volunteers showed no variation in ADC and FA. In patients, extension produced higher ADC in the diseased than in the control segments ($p=0.0045$). The ADC of the affected segments was higher in extension than in the neutral position ($p=0.0030$) or in flexion ($p=0.0002$). The FA was significantly lower in extension in patients at both the control level C2/3 ($p=0.0154$) and the affected segment ($p=0.0187$).

Conclusions Dynamic DTI of the cervical spine is feasible and ADC increased in the patient group in extension. This finding may open a previously unexplored avenue to attempt an earlier identification of myelopathy.

Keywords Dynamic magnetic resonance imaging · Diffusion tensor imaging · Flexion · Extension · Cervical myelopathy

Introduction

The use of T2-weighted magnetic resonance imaging (MRI) is the gold standard for detection of myelopathy in degenerative cervical spinal canal stenosis; however, intramedullary hyperintensity (IHIS) on T2-weighted imaging only has a sensitivity of 61% for the detection of clinical myelopathy compared to a sensitivity of 80% for increased intramedullary apparent diffusion coefficient (ADC) values [1]. The sensitivity of T2-weighted imaging for previously undetected spinal cord compression can be slightly improved by performing dynamic flexion-extension T2-weighted imaging [2]. Moreover, T2 signal hyperintensities may reveal an otherwise undetected myelopathy [3]. While the technique of flexion-extension MRI is not yet in widespread clinical use, its superior sensitivity suggests that it might render T2-weighted imaging modality suitable for the detection of myelopathy.

A diffusion tensor imaging (DTI) sequence performed with extension and flexion of the cervical spine may combine the advantages of the higher sensitivity of DTI with the added sensitivity of a flexion-extension study. Potentially, the appearance of a signal change in a specific position could lead to an earlier detection of myelopathic changes in the spinal cord. In turn, this could facilitate decision-making for clinically symptomatic patients with no clear sign of myelopathy on conventional MRI; however, imaging of the spinal cord presents several challenges, such as

✉ Jatta Berberat
jatta.berberat@ksa.ch

1 Department of Neuroradiology, Cantonal Hospital Aarau, Tellstraße 25, 5001 Aarau, Switzerland

2 Department of Neurosurgery, Cantonal Hospital Aarau, Aarau, Switzerland

3 Department of Neurosurgery, University Medicine Göttingen, Georg-August University, Göttingen, Germany

4 Department of Neurology, Cantonal Hospital Aarau, Aarau, Switzerland

5 Department of Neurosurgery, Hirslanden Clinik, Aarau, Switzerland

spatially inhomogeneous magnetic field environment when in an MRI system, small physical dimensions of the cord cross-section, physiological motion, not to forget the additional scanning time; therefore, DTI is not yet routinely performed in detection of myelopathy. The aim of the current study was to assess the feasibility of flexion-extension DTI as part of a standard cervical spine study in healthy volunteers and patients with clinical symptoms suggesting a potential cervical spinal stenosis.

Materials and Methods

Subjects

This prospective study was approved by the local ethics committee and funded by the institutional research fund (Study no. 1410.000.034). This study was designed as a two-step feasibility study: first, a group of healthy volunteers ($n = 16$) underwent MRI scans in flexion, neutral position and extension. After proving feasibility, MRI scans were performed in patients with cervical complaints ($n = 11$) and a clinical suspicion of degenerative cervical spinal disease. All subjects provided written informed consent for participation in the study. All participants were requested to signal possible tingling, weakness, pain and discomfort during the examination at any time. Healthy volunteers had no prior history of cervical complaints.

Patients with evidence of prior inflammatory nervous system disease ($n = 1$), significant neck trauma ($n = 1$) and prior spinal surgery ($n = 1$) were excluded from the study. Clinical data obtained from the remaining 11 recruited patients included the presence of neck pain, the presence of radicular pain irradiating into the shoulder or upper extremities, duration of symptoms and the modified Japanese Orthopedic Association (mJOA) score [4].

Magnetic Resonance Imaging

Spinal MRI was performed on a 3 T Skyra with 20-channel head- and spine coil (Siemens Healthcare, Erlangen, Germany). The average scan time for all sequences including repositioning of the healthy volunteers was 65 ± 11 min. After completion and analysis of the volunteer part of the study, we shortened the protocol for the comfort of the patients (average 37 ± 9 min which resulted from omitting axial DTI between C2/3 and the affected segment). The imaging protocol consisted of the following sequences: sagittal T2-weighted turbo spin echo (TSE) with the following parameters: acquisition time (TA) of 3:20 min, repetition time (TR) of 3500 ms, echo time (TE) of 126 ms, echo train length of 19, slice thickness of 3 mm and 1 average along the whole length of the cervical spinal cord. The DTI was obtained in axial and sagittal directions in healthy volunteers, whereas DTI of the patient group was obtained only in sagittal direction (axial scans were obtained arbitrarily at levels C2/3 and C4/5). The sagittal scan covered the whole cervical spinal cord. Axial images were executed perpendicular to the spinal cord using the RESOLVE diffusion sequence [5], permitting acquisition of multishot diffusion-weighted echoplanar scans (TA = 3 : 40 min, TR = 1800 ms, TE = 62 ms, 3 mm slice thickness, 2 averages, b values of 0 and 750 s/mm^2). A sagittal diffusion-weighted scan followed (TA = 4 min, TR = 1700 ms, TE = 62 ms, 3 mm slice thickness, 2 averages, b values of 0 and 750 s/mm^2). The dynamic examination was performed with as much active neck flexion as the participant could achieve without discomfort. Head and shoulders were stabilized using padding. We did not attempt to achieve standard predetermined positions thus allowing each subject to find a comfortable position within the head coil. All sequences were performed in flexion, extension and neutral neck positions.

The FA and ADC values were automatically created by the Siemens scanner based on a deterministic fixed step tracking algorithm using the directional information described by the diffusion tensor. Additionally, it also uses a Gaussian model for DTI, where the model spreads several seeds per voxel and takes the neighboring DTI voxel information into account by interpolation [6]. Furthermore, data quality was checked continuously. There were no outliers requiring evaluation of data quality. No subjects were excluded on grounds of missing or implausible DTI data.

Image Analysis

Experienced neuroradiologists (1 >20 years, 1 >5 years experience) screened the sagittal T2-weighted images for possible cervical stenosis, spinal cord atrophy, focal or diffuse signal abnormalities or nerve root compressions. Measurements were performed in a team and possible incongruences in defining the area of interest were resolved by mutual agreement. Sagittal canal diameters, as well as anterior and posterior length of spinal cord from the lower endplate of C2 to the lower endplate of C7, were measured. Central canal compression was graded according to the Muhle classification as described by Bartlett et al. [2]: normal (0): cerebrospinal fluid (CSF) visible dorsal or ventral, not indented on sagittal, and normal shape on axial: equivocal (1): no CSF visible dorsal and ventral on sagittal and/or axial, but not indented or displaced on sagittal (i. e. "nipped"), or atrophic or flattened but CSF visible dorsal and/or ventral: compressed (2): no CSF dorsal and ventral plus indented or displaced on sagittal, and/or flattened on axial. The angle between a line parallel to the lower endplate C2 to the lower endplate of C7 served as a measure of angulation (Cobb angle; Fig. 1). In the DTI dataset, mean ADC and FA values

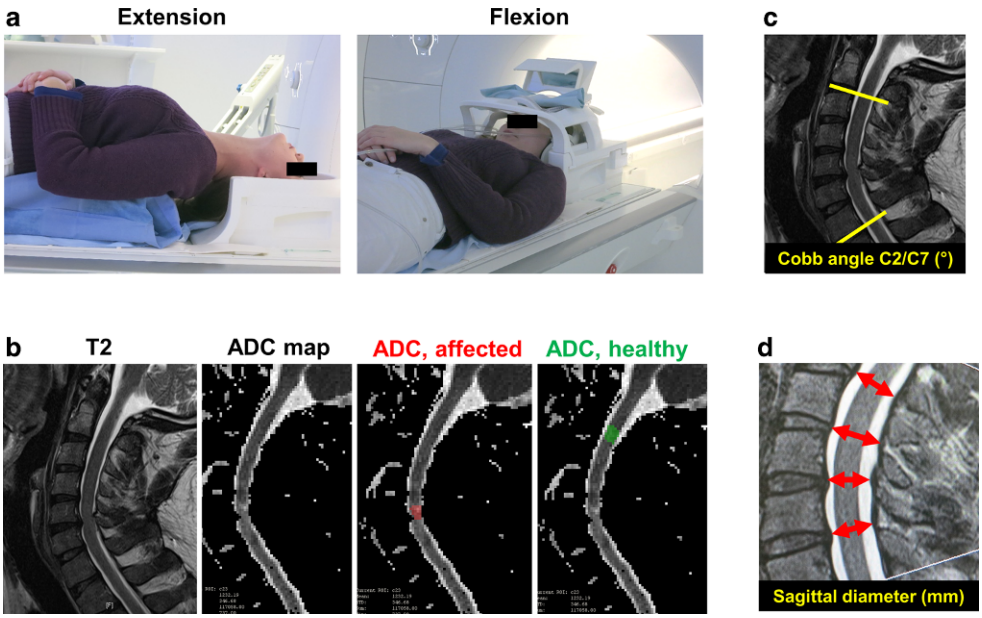

Fig. 1 Positioning and measurements. **a** In order to perform imaging in the extension position, the upper body was slightly elevated with foam padding. Thus, the head was fitted into the head coil in hyperextension ("chin up"). For scanning in the flexion position, the upper body lay flat, allowing inclination of the head ("chin down") using foam padding which was placed in the head coil. **b** Sample images from a patient. T2-weighted imaging demonstrates stenosis at the C5/6 level. Sagittal apparent diffusion coefficient (ADC) maps were used to assess ADC values in the spinal cord at two levels. First, the segment affected by stenosis was measured ("affected", *red region* of interest) by selecting the spinal cord over a length of about 10 mm centered on the disc space. C2/3 ("healthy", *green region* of interest) served as a control level. Fractional anisotropy (FA) values were assess in an analogous manner. **c** The angle between a line parallel to the lower endplate C2 to the lower endplate of C7 served as a measure of angulation (Cobb angle). **d** Sagittal canal diameters (*red arrows*) were measured from the lower endplate of C2 to the lower endplate of C7 at the level of each disc space

were obtained on MATLAB software (Natick, MA, USA). The region of interest for ADC and FA measurements was the spinal cord at a length of 10 mm on a midline section centered on the disc. In healthy volunteers, measurements were performed at the C2/3 and C4/5 levels. In patients, we obtained measurements at a control level (defined as C2/3 which was never affected by stenosis or myelopathy) and at the level of stenosis (Fig. 2).

Statistical Analysis

Statistical analysis was performed using the SPSS 21.0 for Windows statistical package (IBM, Armonk, NY, USA). Mean age, weight, height, BMI and range of motion were compared between healthy volunteer and patient groups. For measurements in healthy subjects, the corresponding index segments C2/3 and C4/5 were chosen for apparent diffusion coefficient (ADC) and fractional anisotropy (FA) assessments on ADC and FA sequences, respectively. In patients, we obtained control values from the unaffected segment (C2/3 in all cases) and compared it to the segment affected by stenosis. The ΔADC and ΔFA values were compared to patients without IHIS. Student's t-test was used to compare the normally distributed data and the Whitney-Mann U-test was used for non-parametric testing in case distribution was non-normal. Sex distribution between groups was compared using a χ^2-test.

The Inter-rater reliability, i. e. the level of agreement between raters, was calculated as percentage agreement. Intraclass correlation (ICC) that reflects the degree of correlation and agreement between the measurements was calculated as follows: ICC = (SD_of_subjects_true_values)²/((SD_of_subjects_true_values)² + (SDS_measurement_error)²).

Results

Basic Parameters

The healthy volunteer group consisted of 16 subjects with a mean age of 37.8 ± 17.0 years, 9 (64%) male, average BMI 23.4 ± 6.3 without any prior history of cervical complaints. The patient group included 11 subjects with suspected cervical myelopathy who underwent MRI scans for diagnostic reasons. Patient mean age was 55.0 ± 14.2 years, 5 subjects (36%) were male and the average BMI was 27.7 ± 6.4. Except for lower age in the healthy volunteer compared to the patient group ($p = 0.01$, Table 1), the epidemiological and clinical baseline characteristics were well matched. Flexion-extension MRI of the cervical spine was well tolerated by all participants. There were no complaints except for

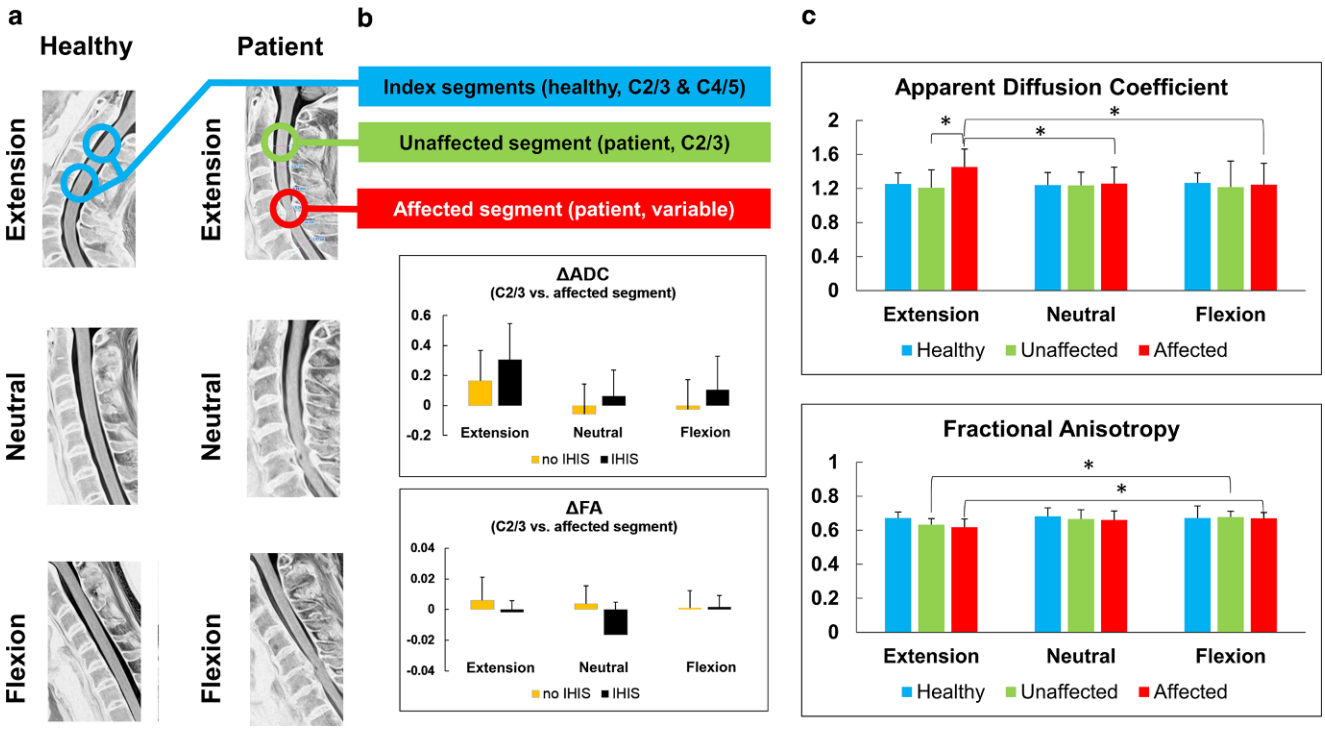

Fig. 2 Dynamic diffusion tensor imaging (DTI) of the cervical spine. **a** Structural T2-weighted magnet resonance imaging is depicted for a healthy volunteer (*left*) and for a patient (*right*) in extension, neutral position and flexion. For measurements in healthy subjects ($n = 16$; *blue bars*), the corresponding index segments C2/3 and C4/5 were chosen for apparent diffusion coefficient (ADC) and fractional anisotropy (FA) assessments on ADC and FA sequences, respectively. In patients ($n = 11$), we obtained control values from the unaffected segment (C2/3 in all cases; *green bars*) and compared it to the segment affected by stenosis (segments C3/4, C4/5, C5/6 or C6/7; *red bars*). **b** Out of 11 patients 6 (55%) had intramedullary hyperintense signals (IHIS; *orange bars*) at the affected segments. Their ΔADC- and ΔFA-values were compared to patients without IHIS (*black bars*; error bar: standard deviation). No significant difference was found in ADC- and FA-values between the groups of patients with and without IHIS. **c** In healthy volunteers (*blue bars*), ADC- and FA-values were highly reproducible, within very close limits, and did not change during the extension-neutral position-flexion paradigm. In patients, however, extension led to two important changes: First, extension produced higher ADC-values in the affected segment (*red bars*) than in the control segment (*green bars*; $p = 0.0045$). Second, ADC-values of the affected segments were higher in extension than in the neutral position ($p = 0.0030$) or in flexion ($p = 0.0002$). FA values were significantly lower in extension in patients at both the control level C2/3 ($p = 0.0154$) and the affected segment ($p = 0.0187$)

Table 1 Baseline characteristics and range of motion (between-group comparison of continuous variables was performed using t-tests; sex distribution was compared using χ^2-tests; values are presented as mean ± SD)

	Healthy volunteers ($n = 16$)	Patients ($n = 11$)	p-value
Age (years)	37.8 ± 17.0	55.0 ± 14.2	*0.01*
Male sex (n, %)	9 (64.3%)	5 (35.7%)	0.58
Weight (kg)	71.2 ± 17.9	85.1 ± 25.9	0.16
Height (cm)	174.8 ± 12.1	174.1 ± 11.6	0.91
Body mass index (kg/m^2,)	23.4 ± 6.2	27.7 ± 6.4	0.15
Range of motion (°)	45.6 ± 17.4	36.0 ± 11.6	0.12
Angle extension (°)	39.9 ± 12.0	29.1 ± 9.1	*0.02*
Angle neutral position (°)	17.7 ± 12.1	14.9 ± 9.5	0.53
Angle flexion (°)	–5.6 ± 12.9	–6.9 ± 13.1	0.80

temporary tingling in the upper extremities of one healthy participant, which resolved within minutes after the examination.

Clinical Parameters

In the patient group, neck pain was the predominant symptom in 9 out of 11 patients (81.8%) and radicular pain was the reason for imaging in 1 case (9.1%). A clinical suspicion of myelopathy was present in 4 patients (38.4%). The av-

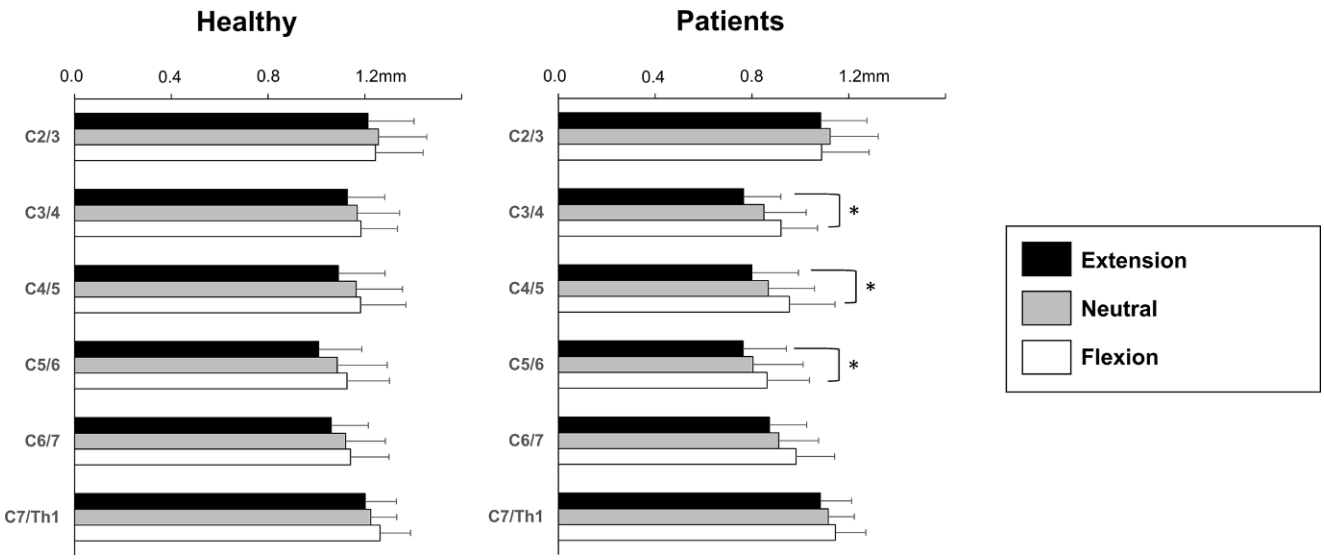

Fig. 3 Sagittal diameter of the spinal canal. Based on T2-weighted imaging, we measured the sagittal diameter of the spinal canal at the level of each disc (space available for the cord, shown in mm). The left bar graph depicts average values for healthy volunteers ($n = 16$), the right side shows values of patients with cervical spinal complaints ($n = 11$). Sagittal spinal canal diameters (space available for the cord) were compared across groups and positions. All spinal canal diameters were lower in patients than healthy volunteers (all p-values <0.05). In healthy volunteers, no significant spinal narrowing was produced in extension position. In patients, we found significantly lower diameters in extension compared to flexion at levels C3/4, C4/5 and C5/6 (p-values 0.041, 0.015 and 0.041, respectively)

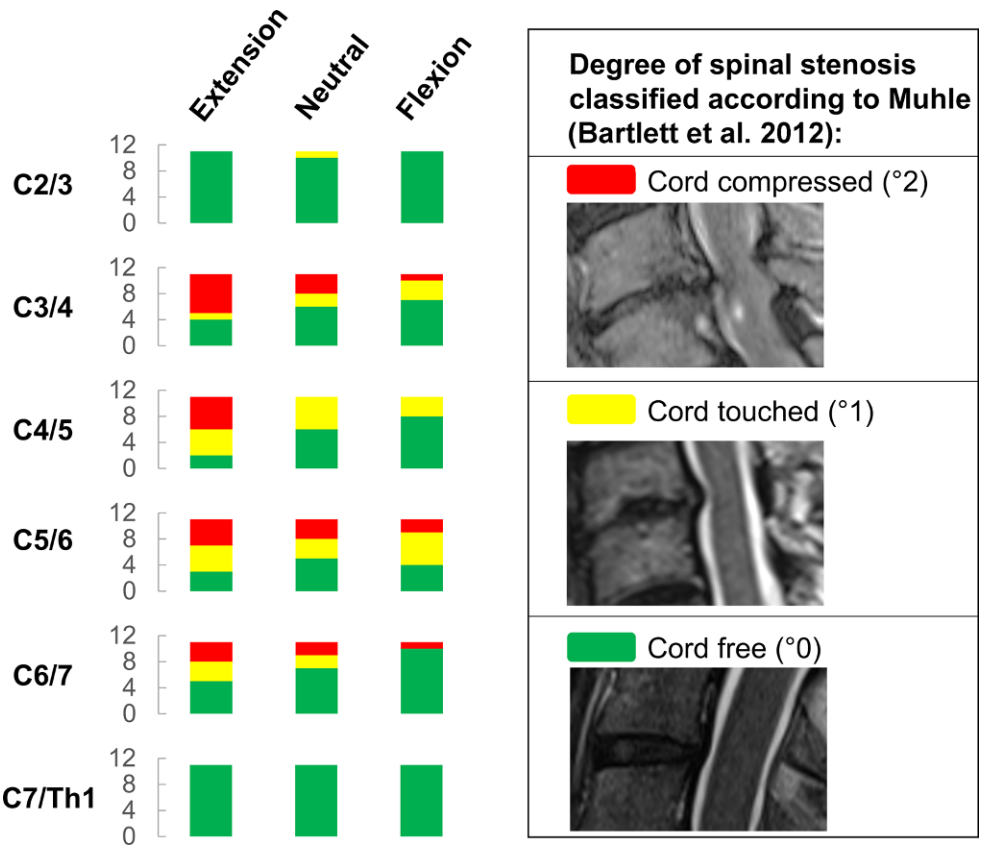

Fig. 4 Proportion of stenotic segments during extension, neutral position and flexion. We graded cervical spinal canal stenosis in patients ($n = 11$) using the Muhle scale as employed by Bartlett et al. [2] based on sagittal T2-weighted imaging. All segments with the exception of C2/3 and C7/Th1 showed dynamic increases in stenosis with increasing degree of extension. *Y-axis* number of patients, *Red bars* severe stenosis with cord compression, *Yellow bars* cord touched with no visible cerebrospinal fluid layer on one side, *Green bars* cord surrounded by cerebrospinal fluid on both sides

Table 2 Diffusion weighted imaging parameters (values are presented as mean ± SD)

	Healthy (C2/3)		Patient (unaffected level, C2/3)		Patient (affected level)	
	ADC	FA	ADC	FA	ADC	FA
Extension	1.254 ± 0.131	0.672 ± 0.035	1.209 ± 0.210	0.633 ± 0.035	1.454 ± 0.209	0.617 ± 0.049
Neutral	1.239 ± 0.150	0.682 ± 0.050	1.235 ± 0.158	0.666 ± 0.054	1.257 ± 0.194	0.660 ± 0.053
Flexion	1.266 ± 0.116	0.672 ± 0.071	1.216 ± 0.306	0.678 ± 0.033	1.246 ± 0.251	0.671 ± 0.033

ADC apparent diffusion coefficient, *FA* fractional anisotropy

erage duration of symptoms was 37.8 ± 51.2 weeks (range: 2–144 weeks). The mean mJOA score was 16.3 ± 1.6.

Imaging Findings

Although the overall range of motion was not different between the two groups, extension was limited to an average of 29° ± 9 in patients compared to 40° ± 12 in volunteers ($p = 0.02$; Table 1).

Sagittal spinal canal diameters (space available for the cord) were compared across the groups and positions (Fig. 3). All spinal canal diameters were lower in patients than in healthy volunteers ($p < 0.05$). No significant spinal cord narrowing was produced in extension in healthy volunteers. In patients, significantly lower diameters in extension compared to flexion at levels C3/4, C4/5 and C5/6 ($p < 0.05$) were observed. In accordance, the degree of spinal canal stenosis according to the Muhle classification increased with the extension position (Fig. 4). The IHIS on T2-weighted imaging was found in 6 patients (55%) and was generally identifiable in all 3 positions.

Apparent Diffusion Coefficient Maps and Fractional Anisotropy

In healthy volunteers, ADC and FA values were highly reproducible, within very close limits, and did not change during the dynamic examination (Table 2). Average ADC values were 1.25 ± 0.1 (extension), 1.24 ± 0.2 (neutral) and 1.27 ± 0.1 (flexion) and FA values were 0.67 ± 0.04 (extension), 0.68 ± 0.05 (neutral) and 0.67 ± 0.07 (flexion). In patients, however, extension led to two important changes: first, extension produced higher ADC values in the diseased segment than in the control segment (1.21 ± 0.2 at the reference level compared to 1.45 ± 0.2 at the affected level; $p = 0.0045$) and second, ADC values of the affected segments were higher in extension (1.45 ± 0.2) than in the neutral position (1.26 ± 0.2; $p = 0.0030$) or in flexion (1.25 ± 0.3; $p = 0.0002$). The FA values were significantly lower in extension compared to flexion in patients at both the control level C2/3 (0.63 ± 0.04 versus 0.68 ± 0.03; $p = 0.0154$) and the affected segment (0.62 ± 0.05 versus 0.67 ± 0.03; $p = 0.0187$).

Since 6 out of 11 patients (55%) had T2-weighted IHIS at the diseased segments, we performed a subgroup analysis to assess whether DTI parameters differ because of the observed signal intensity changes on T2-weighted imaging. Thus, ΔADC and ΔFA values from patients with and without IHIS were compared. No significant difference was found in ADC and FA values between the groups of patients with and without IHIS (Fig. 1b).

Since 6 out of 11 patients (55%) had T2-weighted IHIS at the diseased segments, we performed a subgroup analysis to assess whether DTI parameters differed based on the observed signal intensity changes on T2-weighted imaging. Thus, ΔADC and ΔFA values from patients with and without IHIS were compared. Values of ΔFA ± SD: no IHIS group ($n = 5$): extension 0.006 ± 0.015, neutral: 0.004 ± 0.011, flexion: 0 ± 0.012; IHIS group ($n = 6$): extension –0.002 ± 0.007, neutral –0.017 ± 0.022, flexion: 0.002 ± 0.008. Values of ΔADC ± SD: no IHIS group ($n = 5$): extension 0.164 ± 0.204, neutral –0.058 ± 0.200, flexion: –0.026 ± 0.197; IHIS group ($n = 6$): extension 0.307 ± 0.240, neutral 0.062 ± 0.175, flexion: 0.103 ± 0.225. No significant differences were found in ADC and FA values between the groups of patients with and without IHIS (Fig. 1b).

Two observers re-analyzed blinded 4 patients and both repeated the measurements two times. Results were compared to the original measurement done together in the first phase of the study. Interrater agreement for all the measurements was between 79% and 92%. Intraclass correlation (ICC) yielded to ICC = 0.9, reflecting an excellent agreement between the measurements.

Discussion

This prospective study assessed the feasibility of flexion-extension DTI of the cervical spine with a conventional head and neck coil. Our main finding was that kinematic DTI of the cervical spine can be tolerated in both healthy volunteers and, more importantly, patients with suspected disease of the cervical spine. The flexion-extension paradigm did not require any changes in our scanning equipment and, once streamlined, was performed in little more than half an hour including a routine cervical spine study. The exten-

sion paradigm performed in this study confirmed previous reports about visualizing otherwise inapparent segmental stenosis on T2-weighted imaging [7], but without the need for an upright MRI. Finally, we analyzed DTI values of the spinal cord in flexion, neutral position and extension and found distinct differences: measurements in healthy volunteers demonstrated that DTI values were highly reproducible and remained stable in all the three neck positions. In patients however, at stenotic segments, neck extension produced a change in spinal cord measurements compared to neutral position or flexion: ADC values increased in the extension position compared to the neutral and flexion position. The FA values in extension were lower compared to the flexion position.

Kinematic DTI

Diffusion tensor imaging produces a three-dimensional water diffusion model that reflects the structural continuity of the white matter fibers [8]. The loss of signal intensity can be measured in each voxel by the apparent diffusion coefficient (ADC). If the white matter tracts are disrupted or the permeability of axonal membranes is increased, the ADC will increase. Fractional anisotropy, on the other hand, is a measure of the directional dependence of the ADC, which decreases with WMT disruption [9].

In the patient group, ADC values significantly increased in extension. The degree of stenosis increased and space available for the cord decreased in extension. This "compression strain" is most prominent in the mid-cervical segments and was well delineated in our cohort. Cord compression in extension may provoke increased membrane permeability and lead to increased ADC values. The rise in ADC due to a positional change may reflect that ADC is sensitive to minute, potentially reversible changes within the spinal cord. As postulated recently in anecdotic cases with reversible symptoms, increases in ADC may indicate potentially reversible spinal cord injury [10]. The FA values were lower in extension compared to flexion in our patient cohort, showing that anisotropy may be affected as well.

Our values for FA and ADC in the neutral position are within the range of recently published series [11, 12]. These parameters remained stable in flexion and extension when measured in healthy subjects. In the neutral neck position, a correlation between normal DTI properties and preserved neurological function has been shown in several studies [13–15]. Decreased FA and increased ADC values are associated with clinical findings of neurological impairment [13, 16, 17] and potentially worse postoperative outcomes [12]. The decrease in FA and a rise in ADC provoked by a simple hyperextension of the neck in a conventional MRI scanner may serve as tool in identifying spinal cord changes which remained undetected in the neutral position in patients.

T2-Weighted Imaging

Cervical spondylotic myelopathy can be associated with significant instability of the cervical spine. Dynamic flexion-extension images may therefore reveal significant compression of neural structures despite inconclusive conventional imaging in the neutral position. In addition to a potentially visible compression, Zhang et al. demonstrated that flexion maneuver of the cervical spine may reveal T2-signal changes in patients with spondylotic changes in the cervical spine [3]. The use of such a flexion-extension paradigm in T2-weighted imaging increased the diagnosed rate of cord compression from 12% to 26% in neutral position. In hyperextension, the rate of spinal cord impingement reached 76%. An IHIS was found as a sign of myelopathy in flexion in 40% and conversely in extension only in 14%. The authors concluded that in some patients, only the flexed cervical spine allows sufficient decompression of the spinal cord to reveal a IHIS, and that IHIS may be masked by compression of the cord parenchyma in the neutral or extended position.

The T2-weighted IHIS reflects cord edema or myelomalacia. Therefore, we would have expected to find a significant difference in ADC values between patients at segments with and without IHIS. In our study however, the subgroup analysis of ADC values in the presence of an IHIS was inconclusive, which may be explained by two factors: first, this feasibility study is underpowered to show correlations in imaging parameters, especially in subgroups with low patient numbers. Thus, potentially significant alterations in ADC or FA may have remained undetected. Second, ADC values may be high at some point in myelopathy (supposedly early on) and lower in the later stages [10], preventing us to detect a net difference despite the possible presence of ADC changes in the individual patient. Not only absolute values, but also appearance of fiber continuity on DTI is associated with certain clinical parameters such as the mJOA in cervical spondylotic myelopathy [18].

There is a long-standing debate about whether kinematic imaging is a prerequisite for routine imaging or simply an exceptional add-on. The most widely adopted kinematic study, flexion-extension x-rays of the cervical spine, even though an established technique, is still scrutinized for issues such as lack of objective criteria and a limited interobserver reliability [19]. Kinematic computed tomography-based myelography provides more detailed information and is therefore used by some centers as an adjunct in surgical decision-making for complex cases. Biometric measurements using kinematic computed tomography-based myelography in healthy volunteers and patients yielded results on spinal canal content similar to our findings [20]; however, its invasiveness and radiation exposure are important limitations and is therefore reserved for pre-surgery can-

didates under specific conditions, i.e. in the case of contraindications to MRI. The use of kinematic MRI in cervical spondylotic myelopathy may be useful in identifying an otherwise undetected narrow spinal canal in one out of five cases [21]. We demonstrated that the use of kinematic MRI is well tolerated. It can be applied in a standard MRI with a conventional head/neck coil without investing in additional equipment. We believe that our data support adding the extra effort for the potential benefit of obtaining a diagnosis in selected patients with moderate spinal canal narrowing on conventional MRI but otherwise severe symptoms. The extension position is possibly the most sensitive tool to detect an occult spinal canal stenosis. It remains to be elucidated whether the flexion position adds valuable information. Information on posture, the range of motion and instability is probably still best obtained using conventional flexion-extension x-rays.

Other Applications of DTI

The use of DTI is appealing for two reasons. First, by returning quantitative instead of mere "visual" values, it might serve as an objective tool for the detection of spinal cord pathology in patients with cervical spondylosis. Second, it reflects the presence of microstructural alterations with respect to the spatial distribution of white matter tracts. The finding that early myelopathic changes are more readily detected by DTI than by the previous gold-standard of T2-weighted imaging fueled hopes for a utility in clinical practice [1].

After spinal trauma, ADC has the highest sensitivity to detect pathological spinal cord changes [22]. In patients suffering from multiple sclerosis with spinal cord affection, characteristic decreases in FA were detected which may be related to disease subtype and progression [23]. Aside from diagnostic applications, DTI can be a useful planning tool: from a surgical point of view, the visualization of fibers using tractography can guide surgeons in deciding how a spinal cord tumor displaces white matter tracts [24]. Thus, the safest entry side or zone into the spinal cord for tumor resection can be defined with the help of DTI.

Technical Challenges

Imaging of the spinal cord presents several challenges [25], such as (1) spatially inhomogeneous magnetic field environment when in an MRI system, (2) small physical dimensions of the cord cross-section, and (3) physiological motion. To overcome these problems, the imaging area was carefully shimmed and sagittal scans were acquired [26–28]. This allowed us to take advantage of the small dimensions and typically low curvature of the spinal cord in the right-left direction. Moreover, this measure kept acquisition time low and patient comfort at its maximum; however, when scanning the volunteers, we obtained axial DTI of the spinal cord as well, since it reveals more detailed information on fiber tracts [29–33]. Since the physiological motion may bias ADC estimation [25] and create ghosting artifacts [34], extra care was taken while analyzing the images to avoid possible artefacts. Further, the small physical dimensions of the cord may contribute to partial volume effects, which are accentuated in the cord by the proximity of white matter tracts to the surrounding cerebrospinal fluid (CSF) [35]. Care was taken to analyze a slice with a clean cord appearance. Since standard DWI and DTI imaging sequences are based on echo-planar imaging (EPI), and are sensitive to the poor magnetic field homogeneity in the spinal cord [36], we chose to use the RESOLVE (multishot echoplanar diffusion weighted imaging) sequence, which offers diffusion-weighted images with a higher level of detail than that offered by current single-shot EPI scans. For tractography studies isotropic voxels are preferred [37], as also implied in our study ($3 \times 3 \times 3\,mm^3$). Lastly, the optimal b-value for spinal cord imaging varies between 700–1500 s/mm^2. We chose $b = 750$ with the advantage of a shorter echo time (TE) and therefore an increased SNR. The recommended number of directions for robust DTI estimation is at least 20 icosahedral directions [38], in our study we used 30 diffusion directions.

Limitations of the Study

The cervical spinal cord requires imaging with a high spatial resolution to provide meaningful values. Even minimal motion due to heart beat and breathing may induce motion artefacts. Susceptibility artefacts within the spinal canal are another source of reduced signal in the cervical spine [1, 39, 40]. In recent years, technical improvements have partly resolved some of the above issues, resulting in acceptable image quality [41]; however, a definitive pixel or voxel-wise identification of white matter tracts within the spinal cord is not possible in every individual case despite the use of a 3 T scanner. This difficulty may become even more apparent when spinal cord anatomy is distorted due to compression in spondylotic myelopathy.

The main limitation of the study was the fact that the patient population was not age-matched with the healthy volunteer cohort. There are two reasons for this: first, imaging of volunteers including the feasibility step was performed first. Therefore, the mean age of the patient group was not known until after completion of the second part of the study. We are aware that this might be viewed as an important limitation since cervical spinal stenosis is classically a disease of the elderly. Nonetheless, the feasibility of the protocol was demonstrated in both groups. Thus, we are confident that this aspect of the pilot study is not altered by the age

mismatch. The observed intramedullary signal alteration in the stenotic segments in extension should equally be independent of the age mismatch since we also measured the unaffected reference segment of a patient (C2/3). Therefore, patients served as their own controls. Finally, an internal analysis showed no association of FA and ADC values at the control level C2/3 with age.

Due to the small sample size, we cannot conclude that the study findings of ADC or FA alterations correlate with any kind of cervical spinal pathology. Since this study served as a pilot project, it demonstrated feasibility rather than actual correlations of imaging with clinical findings.

Conclusion

This study demonstrates that flexion-extension MRI including DTI is feasible, and it can be performed in a conventional scanner with head and neck coil in little more than 30 min; however, larger studies are needed to confirm its utility and safety in routine examination settings. The use of MRI in extension leads to structural narrowing of the spinal canal and exerts a stress on the spinal cord. In our patient population, this resulted in a marked increase of ADC values in extension. Further studies with larger sample size and a longitudinal design will be needed to address the question whether ADC changes in extension may represent an early imaging biomarker of myelopathy.

Conflict of interest B. Schatlo, L. Remonda, P. Gruber, J. Fandino, V. Rohde, A.-R Fathi and J Berberat declare that they have no competing interests.

References

1. Demir A, Ries M, Moonen CT, Vital JM, Dehais J, Arne P, Caillé JM, Dousset V. Diffusion-weighted MR imaging with apparent diffusion coefficient and apparent diffusion tensor maps in cervical spondylotic myelopathy. Radiology. 2003;229:37–43.
2. Bartlett RJ, Hill CA, Rigby AS, Chandrasekaran S, Narayanamurthy H. MRI of the cervical spine with neck extension: is it useful? Br J Radiol. 2012;85:1044–51.
3. Zhang L, Zeitoun D, Rangel A, Lazennec JY, Catonné Y, Pascal-Moussellard H. Preoperative evaluation of the cervical spondylotic myelopathy with flexion-extension magnetic resonance imaging: about a prospective study of fifty patients. Spine (Phila Pa 1976). 2011;36:E1134–9.
4. Benzel EC, Lancon J, Kesterson L, Hadden T. Cervical laminectomy and dentate ligament section for cervical spondylotic myelopathy. J Spinal Disord. 1991;4:286–95.
5. Tullos H, Dale B, Bidwell G, Perkins E, Raucher D, Khan M, James J. Multi-shot RESOLVE compared to single-shot EPI diffusion-weighted MR imaging acquisition scheme. Med Phys. 2012;39:3640.
6. Basser PJ, Pajevic S, Pierpaoli C, Duda J, Aldroubi A. A in vivo fiber tractography using DT-MRI data. Magn Reson Med. 2000;44:625–32.
7. Jinkins JR, Dworkin JS, Damadian RV. Upright, weight-bearing, dynamic-kinetic MRI of the spine: initial results. Eur Radiol. 2005;15:1815–25.
8. Hagmann P, Jonasson L, Maeder P, Thiran JP, Wedeen VJ, Meuli R. Understanding diffusion MR imaging techniques: from scalar diffusion-weighted imaging to diffusion tensor imaging and beyond. Radiographics. 2006;26(Suppl 1):S205–23.
9. Basser PJ, Mattiello J, LeBihan D. MR diffusion tensor spectroscopy and imaging. Biophys J. 1994;66:259–67.
10. Endo T, Suzuki S, Inoue T, Utsunomiya A, Uenohara H, Tominaga T. Prediction of neurological recovery in spontaneous spinal epidural hematoma using apparent diffusion coefficient values. Spinal Cord. 2014;52:729–33.
11. Uda T, Takami T, Tsuyuguchi N, Sakamoto S, Yamagata T, Ikeda H, Nagata T, Ohata K. Assessment of cervical spondylotic myelopathy using diffusion tensor magnetic resonance imaging parameter at 3.0 tesla. Spine (Phila Pa 1976). 2013;38:407–14.
12. Rindler RS, Chokshi FH, Malcolm JG, Eshraghi SR, Mossa-Basha M, Chu JK, Kurpad SN, Ahmad FU. Spinal diffusion tensor imaging in evaluation of preoperative and postoperative severity of cervical spondylotic myelopathy: systematic review of literature. World Neurosurg. 2017;99:150–8.
13. Qian W, Chan Q, Mak H, Zhang Z, Anthony MP, Yau KK, Khong PL, Chan KH, Kim M. Quantitative assessment of the cervical spinal cord damage in neuromyelitis optica using diffusion tensor imaging at 3 Tesla. J Magn Reson Imaging. 2011;33:1312–20.
14. Ellingson BM, Kurpad SN, Schmit BD. Functional correlates of diffusion tensor imaging in spinal cord injury. Biomed Sci Instrum. 2008;44:28–33.
15. Kerkovský M, Bednarík J, Dušek L, Sprláková-Puková A, Urbánek I, Mechl M, Válek V, Kadanka Z. Magnetic resonance diffusion tensor imaging in patients with cervical spondylotic spinal cord compression: correlations between clinical and electrophysiological findings. Spine (Phila Pa 1976). 2012;37:48–56.
16. Budzik JF, Balbi V, Le Thuc V, Duhamel A, Assaker R, Cotten A. Diffusion tensor imaging and fibre tracking in cervical spondylotic myelopathy. Eur Radiol. 2011;21:426–33.
17. Chang Y, Jung TD, Yoo DS, Hyun JK. Diffusion tensor imaging and fiber tractography of patients with cervical spinal cord injury. J Neurotrauma. 2010;27:2033–40.
18. Wang K, Chen Z, Zhang F, Song Q, Hou C, Tang Y, Wang J, Chen S, Bian Y, Hao Q, Shen H. Evaluation of DTI parameter ratios and diffusion tensor tractography grading in the diagnosis and prognosis prediction of cervical spondylotic myelopathy. Spine (Phila Pa 1976). 2017;42:E202–10.
19. Taylor M, Hipp JA, Gertzbein SD, Gopinath S, Reitman CA. Observer agreement in assessing flexion-extension X-rays of the cervical spine, with and without the use of quantitative measurements of intervertebral motion. Spine J. 2007;7:654–8.
20. Ishida Y, Suzuki K, Ohmori K. Dynamics of the spinal cord: an analysis of functional myelography by CT scan. Neuroradiology. 1988;30:538–44.
21. Xu N, Wang S, Yuan H, Liu X, Liu Z. Does dynamic supine magnetic resonance imaging improve the diagnostic accuracy of cervical spondylotic myelopathy? A review of the current evidence. World Neurosurg. 2017;100:474–9.
22. Shanmuganathan K, Gullapalli RP, Zhuo J, Mirvis SE. Diffusion tensor MR imaging in cervical spine trauma. AJNR Am J Neuroradiol. 2008;29:655–9.
23. Agosta F, Absinta M, Sormani MP, Ghezzi A, Bertolotto A, Montanari E, Comi G, Filippi M. In vivo assessment of cervical cord damage in MS patients: a longitudinal diffusion tensor MRI study. Brain. 2007;130:2211–9.
24. Ducreux D, Lepeintre JF, Fillard P, Loureiro C, Tadié M, Lasjaunias P. MR diffusion tensor imaging and fiber tracking in 5 spinal cord astrocytomas. AJNR Am J Neuroradiol. 2006;27:214–6.

25. Stroman PW, Wheeler-Kingshott C, Bacon M, Schwab JM, Bosma R, Brooks J, Cadotte D, Carlstedt T, Ciccarelli O, Cohen-Adad J, Curt A, Evangelou N, Fehlings MG, Filippi M, Kelley BJ, Kollias S, Mackay A, Porro CA, Smith S, Strittmatter SM, Summers P, Tracey I. The current state-of-the-art of spinal cord imaging: methods. Neuroimage. 2014;84:1070–81.
26. Kharbanda HS, Alsop DC, Anderson AW, Filardo G, Hackney DB. Effects of cord motion on diffusion imaging of the spinal cord. Magn Reson Med. 2006;56:334–9.
27. Shen H, Tang Y, Huang L, Yang R, Wu Y, Wang P, Shi Y, He X, Liu H, Ye J. Applications of diffusion-weighted MRI in thoracic spinal cord injury without radiographic abnormality. Int Orthop. 2007;31:375–83.
28. Thurnher MM, Bammer R. Diffusion-weighted MR imaging (DWI) in spinal cord ischemia. Neuroradiology. 2006;48:795–801.
29. Cohen-Adad J, El Mendili MM, Lehéricy S, Pradat PF, Blancho S, Rossignol S, Benali H. Demyelination and degeneration in the injured human spinal cord detected with diffusion and magnetization transfer MRI. Neuroimage. 2011;55:1024–33.
30. Ellingson BM, Ulmer JL, Kurpad SN, Schmit BD. Diffusion tensor MR imaging in chronic spinal cord injury. AJNR Am J Neuroradiol. 2008;29:1976–82.
31. Kim JH, Loy DN, Liang HF, Trinkaus K, Schmidt RE, Song SK. Noninvasive diffusion tensor imaging of evolving white matter pathology in a mouse model of acute spinal cord injury. Magn Reson Med. 2007;58:253–60.
32. Smith SA, Jones CK, Gifford A, Belegu V, Chodkowski B, Farrell JA, Landman BA, Reich DS, Calabresi PA, McDonald JW, van Zijl PC. Reproducibility of tract-specific magnetization transfer and diffusion tensor imaging in the cervical spinal cord at 3 tesla. NMR Biomed. 2010;23:207–17.
33. Wilm BJ, Gamper U, Henning A, Pruessmann KP, Kollias SS, Boesiger P. Diffusion-weighted imaging of the entire spinal cord. NMR Biomed. 2009;22:174–81.
34. Clark CA, Barker GJ, Tofts PS. Improved reduction of motion artifacts in diffusion imaging using navigator echoes and velocity compensation. J Magn Reson. 2000;142:358–63.
35. Nunes RG, Jezzard P, Behrens TE, Clare S. Self-navigated multishot echo-planar pulse sequence for high-resolution diffusion-weighted imaging. Magn Reson Med. 2005;53:1474–8.
36. Heidemann RM, Ozsarlak O, Parizel PM, Michiels J, Kiefer B, Jellus V, Müller M, Breuer F, Blaimer M, Griswold MA, Jakob PM. A brief review of parallel magnetic resonance imaging. Eur Radiol. 2003;13:2323–37.
37. Jones DK, Williams SC, Gasston D, Horsfield MA, Simmons A, Howard R. Isotropic resolution diffusion tensor imaging with whole brain acquisition in a clinically acceptable time. Hum Brain Mapp. 2002;15:216–30.
38. Jones DK. The effect of gradient sampling schemes on measures derived from diffusion tensor MRI: a Monte Carlo study. Magn Reson Med. 2004;51:807–15.
39. Agosta F, Benedetti B, Rocca MA, Valsasina P, Rovaris M, Comi G, Filippi M. Quantification of cervical cord pathology in primary progressive MS using diffusion tensor MRI. Neurology. 2005;64:631–5.
40. Elshafiey I, Bilgen M, He R, Narayana PA. In vivo diffusion tensor imaging of rat spinal cord at 7 T. Magn Reson Imaging. 2002;20:243–7.
41. Petersen JA, Wilm BJ, von Meyenburg J, Schubert M, Seifert B, Najafi Y, Dietz V, Kollias S. Chronic cervical spinal cord injury: DTI correlates with clinical and electrophysiological measures. J Neurotrauma. 2012;29:1556–66.